IJC
International Journal of Cancer

Viral load, gene expression and mapping of viral integration sites in HPV16-associated HNSCC cell lines

Nadine C. Olthof[1,2]* Christian U. Huebbers[3]* Jutta Kolligs[3] Mieke Henfling[2] Frans C.S. Ramaekers[2] Iris Cornet[1,4] Josefa A. van Lent-Albrechts[5] Alexander P.A. Stegmann[5] Steffi Silling[6] Ulrike Wieland[6] Thomas E. Carey[7] Heather M. Walline[7] Susanne M. Gollin[8] Thomas K. Hoffmann[9] Johan de Winter[10] Bernd Kremer[1] Jens P. Klussmann[11†] and Ernst-Jan M. Speel[2,4†]

[1] Department of Otorhinolaryngology and Head and Neck Surgery, GROW–School for Oncology and Developmental Biology, Maastricht University Medical Centre, The Netherlands
[2] Department of Molecular Cell Biology, GROW–School for Oncology and Developmental Biology, Maastricht University Medical Centre, The Netherlands
[3] Jean-Uhrmacher-Institute for Otorhinolaryngological Research, University of Cologne, Germany
[4] Department of Pathology, GROW–School for Oncology and Developmental Biology, Maastricht University Medical Centre, The Netherlands
[5] Department of Clinical Genetics, GROW–School for Oncology and Developmental Biology, Maastricht University Medical Centre, The Netherlands
[6] Institute of Virology, National Reference Centre for Papilloma- and Polyomaviruses, University Hospital of Cologne, Germany
[7] Department of Otolaryngology, University of Michigan, Ann Arbor, MI
[8] Department of Human Genetics, University of Pittsburgh Graduate School of Public Health and the University of Pittsburgh Cancer Institute, Pittsburgh, PA
[9] Department of Otorhinolaryngology and Head and Neck Surgery, Ulm, Germany
[10] Department of Clinical Genetics, VU University Medical Center, Amsterdam, The Netherlands
[11] Department of Otorhinolaryngology, Head and Neck Surgery, School of Medicine, University Hospital of Giessen, Germany

HPV-related HNSCC generally have a better prognosis than HPV-negative HNSCC. However, a subgroup of HPV-positive tumors with poor prognosis has been recognized, particularly related to smoking, EGFR overexpression and chromosomal instability. Viral integration into the host genome might contribute to carcinogenesis, as is shown for cervical carcinomas. Therefore, all HPV16-positive HNSCC cell lines currently available have been carefully analyzed for viral and host genome parameters. The viral integration status, viral load, viral gene expression and the presence of aneusomies was evaluated in the cell lines UD-SCC-2, UM-SCC-047, UM-SCC-104, UPCI:SCC090, UPCI:SCC152, UPCI:SCC154 and 93VU147T. HPV integration was examined using FISH, APOT-PCR and DIPS-PCR. Viral load and the expression of the viral genes E2, E6 and E7 were determined via quantitative PCR. All cell lines showed integration-specific staining patterns and signals indicating transcriptional activity using FISH. APOT- and DIPS-PCR identified integration-derived fusion products in six cell lines and only episomal products for UM-SCC-104. Despite the observed differences in viral load and the number of viral integration sites, this did not relate to the identified viral oncogene expression. Furthermore, cell lines exhibited EGFR expression and aneusomy (except UPCI:SCC154). In conclusion, all HPV16-positive HNSCC cell lines showed integrated and/or episomal viral DNA that is transcriptionally active, although viral oncogene expression was independent of viral copy number and the number of viral integration sites. Because these cell lines also contain EGFR expression and aneusomy, which are parameters of poor prognosis, they should be considered suitable model systems for the development of new antiviral therapies.

Cancer Cell Biology

Infection with high-risk human papillomavirus (HPV) is a causative factor for the development of several types of neoplasms, including cervical, anogenital and a subset of head and neck cancers. Although most head and neck squamous cell carcinomas (HNSCC) can be attributed to the exposure to environmental factors, such as excessive tobacco and

Key words: APOT-PCR, DIPS-PCR, integration, viral integration, genetic localization

Abbreviations: APOT-PCR: amplification of papillomavirus oncogene transcripts PCR; CIN: cervical intraepithelial neoplasia; DIPS-PCR: detection of integrated papillomavirus sequences PCR; FISH: fluorescence *in situ* hybridization; HNSCC: head and neck squamous cell carcinoma; HPV: human papillomavirus; OSCC: oropharyngeal squamous cell carcinomas

Additional Supporting Information may be found in the online version of this article.

Potential conflicts of interest: none

*N.C.O. and C.U.H. contributed equally to this study as first authors

†J.P.K. and E.-J.M.S. contributed equally to this study as senior authors

DOI: 10.1002/ijc.29112

History: Received 20 Oct 2013; Accepted 3 July 2014; Online 1 Aug 2014

Correspondence to: Christian U. Huebbers, Ph.D., Jean-Uhrmacher-Institute for Otorhinolaryngological Research, University of Cologne, Geibelstrasse 29–31, 50931 Cologne, Germany, Tel.: [4922147897017], Fax: +[49-221-478-97010], E-mail: christian.huebbers@uni-koeln.de

What's new?

High-risk human papillomavirus (HPV) infection is a well-established risk factor for head and neck squamous cell carcinoma (HNSCC) development. It is still unclear however whether viral DNA integration into the host genome plays an important role in HPV carcinogenesis in HNSCC. In this study, seven HPV16-positive HNSCC cell lines showed integrated and/or episomal viral DNA that is transcriptionally active. Both viral load and expression of several viral early genes were variable. Because the cell lines also feature EGFR overexpression and aneusomy, which are parameters of poor prognosis, they may represent suitable model systems for the development of new antiviral therapies.

alcohol use, ~20–25% of these cancers are caused by infection with HPV16. Notably, HPV-induced tumors are preferentially found in the oropharynx, where up to 90% of the malignancies are associated with HPV.[1–3]

Patients with HPV-induced carcinomas display clinical and molecular characteristics that are distinct from those in patients with tobacco- and alcohol-induced tumors. It is now well accepted that patients with HPV-derived tumors have a favourable prognosis, independent of the chosen treatment strategy.[4–6]

As first described by Ang *et al.*,[7] HNSCC can be divided into three risk groups, depending on HPV status, the number of pack-years (<10 vs. >10) of tobacco smoking and nodal stage (N0-N2a vs. N2b-N3). In addition, it was shown that *EGFR* overexpression negatively affects overall survival both in HPV-positive as well as in HPV-negative tumors.[4] Chromosomal instability was also reported to have a negative influence on prognosis, especially in HPV-positive tumors.[8] These data indicate that smoking, advanced nodal stage, *EGFR* overexpression and chromosomal instability are risk parameters for poor prognosis in HPV-associated HNSCC.

From uterine cervical (pre)malignancy models it is hypothesized that integration of HPV into the host genome plays an important role in the carcinogenic process. It correlates with the severity and progression of these lesions and is considered a risk factor for the development of uterine cervical squamous cell carcinoma.[9,10] In addition, a higher viral load is associated with higher grade lesions. It is, however, not possible to predict tumor progression based on the integration status of HPV or the viral load.[11]

HNSCC, in particular oropharyngeal squamous cell carcinomas, are mostly discovered as metastatic disease and data on premalignant lesions are scarce. Therefore limited information is available on the role of viral integration in the development of these tumors. It is hypothesized, however, that viral integration also promotes carcinogenesis in HNSCC, but this is not substantiated by clinical studies on premalignant lesions, as is the case for cervical lesions.

Furthermore, the reported integration percentages in HNSCC vary considerably, ranging from 0% to almost 100% in different publications.[1,12–15] This extreme variation might be explained by the different patient populations studied, the different methods applied to study viral integration and a lack of correlation between these methods.

However, the integration status of the virus can be of significance in relation to treatment. Chang *et al.*[16] and Herdman *et al.*[17] have shown a clear difference in the response of keratinocytes with episomal versus integrated HPV. Using these cell line models it could be shown that interferon therapy can eradicate episomal HPV infection, but leads to a growth advantage for cells containing integrated HPV. This indicates that antiviral therapies might be influenced by the viral integration status. Thus, it is imperative to have a well-characterized model for HPV-associated HNSCC, for which the physical status of the virus is known.

This study presents a detailed analysis of the integration status in 7 HPV-positive HNSCC cell lines established from HPV-induced tumors. The integration status has been assessed using a set of independent techniques, that is, DNA and RNA FISH, APOT- and DIPS-PCR. In addition, the expression levels of the viral genes *E2*, *E6* and *E7* and the expression levels of *EGFR*, as well as the viral load were analyzed.

Material and Methods

Cell lines

Human HPV16-positive HNSCC cell lines were obtained from different sources. Cell lines UPCI:SCC090, UPCI:SCC152 and UPCI:SCC154 were kindly provided by Dr. Susanne Gollin from the University of Pittsburgh, Pittsburgh, PA. The UPCI:SCC152 cell line was established from a recurrence in the patient from which the cell line UPCI:SCC090 was derived.[18] Cell line UD-SCC-2 was a kind gift from Dr. Thomas Hoffmann; present address University of Ulm, Germany.[19] The cell lines UM-SCC-047 and UM-SCC-104 were a kind gift from Dr. Thomas Carey, University of Michigan, Ann Arbor, MI. The cell line 93VU147T was provided by Dr. J.P. de Winter, Free University Medical Centre, Amsterdam, The Netherlands.[20] Clinicopathological data of the patients and tumors from which the cell lines were derived are given in Table 1.

Cell lines UD-SCC-2 and 93VU147T were cultured in MEM (Invitrogen, Carlsbad, CA) containing 10% FCS (Sigma, St Louis, MO), 2 mM glutamine (Invitrogen), 0.1 mM MEM nonessential amino acids (Invitrogen) and 0.005% gentamycin (Eurovet Animal Health BV, Bladel, The Netherlands). The remaining cell lines were cultured in DMEM (Invitrogen) containing the same additives as described above. Cell lines UM-SCC-047, UPCI:SCC090 and UD-SCC-2 were received in 2008 and UM-SCC-104, UPCI:SCC152, UPCI:SCC154 and 93VU147T in 2011 and were frozen immediately upon arrival. All cell lines were confirmed to have unique genotypes, as tested using the ProfilerPlus assay, except the cell lines UPCI:SCC090 and UPCI:SCC152, which shared the same genotype as they are derived from the

Table 1. Characteristics of patients from which the cell lines have been derived

Cell line	UD-SCC-2	UM-SCC-47	UM-SCC-104	UPCI:SCC090	UPCI:SCC152	UPCI:SCC154	93VU147T
M/F	M	M	M	M	M	M	M
Age at diagnosis	58	53	56	46	47	54	58
Smoking	y	y	y	y	y	y	y
Alcohol	y	n.a.	y	y	y	y	y
Primary tumor site	hypo-pharynx	lateral tongue	floor of mouth	base of tongue	hypo-pharynx	tongue	floor of mouth
TNM	T1N3	T3N1M0	T4N2bM0	T2N0	recurrence	T4N2	T4N2
Differentiation	n.a.	M/W	P/M	P	M	n.a.	M

Abbreviations: M: Male; F: Female; n.a.: not available; W: well differentiated; M: medium differentiated; P: poorly differentiated.

same patient (see Supporting Information Table S1). Cell lines in culture were regularly tested for infection with mycoplasma.

The uterine cervical cancer cell lines SiHa and CaSki were used as HPV16- and $p16^{INK4A}$-positive controls in $p16^{INK4A}$ immunostaining and HPV16-specific PCR analysis. The uterine cervical cancer cell line HeLa, the HPV-negative HNSCC cell line UPCI:SCC003 and the osteosarcoma cell line U2OS containing the empty pJ4Ω-vector[21] were used as negative controls in these assays. The latter cell line harbouring HPV16-E2-containing pJ4Ω-vector was used as a positive control for HPV16-E2 RT-PCR and immunohistochemistry.

DNA/RNA extraction

DNA was isolated from cultured cells using QIAamp DNA Blood Mini Kit (Qiagen, Hilden, Germany) as per the manufacturers' instructions. Total RNA was extracted using the RNeasy mini kit (Qiagen) according to the manufacturer's instructions, including DNase treatment. RNA concentration and quality were determined by RNA standard sense chips on a BioRad Experion system (BioRad, Munich, Germany).

HPV DNA PCR

The presence of HPV DNA was detected by PCR using the consensus primer set GP5+/6+,[22] followed by type-specific primers for HPV16 and HPV18. The following primers were used:

Target	Primer	Sequence
HPV16	Forward	5′-ACAGGAGCGACCCAGAAAGTTAC-3′
	Reverse	5′ GCATAAATCCCGAAAAGCAAAGT-3′
HPV18	Forward	5′-CACATTGGAAAAACTAACTAACACACTGG-3′
	Reverse	5′-CAGCTATGTTGTGAAATCGTCGTT-3′

Primers were synthesized by Biolegio BV, Nijmegen, The Netherlands. Five microliter of PCR product were separated on a 1.5 % agarose gel and visualized using GelStar Nucleic Acid Gel Stain (Cambrex Bio Science Rockland).

Viral load

Viral load of HPV16 was determined using real-time fluorescence PCR with type-specific primers and probes as described earlier.[23] Briefly, viral load was expressed as the number of HPV16 DNA copies per *β-globin*-gene copy. Gene copy numbers of *β-globin* were determined using the LightCycler-Control Kit DNA (Roche Molecular Biochemicals) according to the manufacturer's instructions as previously described.[24] Calculation of initial copy numbers in samples was performed by the LightCycler 480 software (Version 1.5) using a standard curve generated with exactly quantified HPV DNA standards (ten-fold dilution series of full length HPV16 plasmid) that were amplified in the same PCR run.[23,24] The analytical sensitivity of the assay was 10 copies of HPV16 standard DNA. A negative control (water or DNA extracted from RTS3B cells that are negative for HPV) was included in each run and never yielded fluorescence signals above the background.[25]

Viral integration analysis

DNA and RNA fluorescence in situ hybridization. HPV16-specific probes were purchased from PanPath, Amsterdam, The Netherlands. BAC-clones, used for colocalization experiments, were grown according to the manufacturer's instructions (BACPAC Resources Centre, Childrens Hospital Oakland Research Institute, Oakland). DNA was isolated using the Nucleobond BAC-100 kit (BioKé, Leiden, The Netherlands). Probes for centromeres (CEPs) 1, 3 and 9 were available in our lab, previously described in Hopman *et al.*[26] Probes and clones were labelled using either the Dignick translation kit or the Biotin-nick translation kit (Roche, Basel, Switzerland), according to the manufacturer's instructions. Labeled CEP probes for CEP17 and CEPX were kindly provided by the Department of Clinical Genetics, Maastricht University Medical Centre, Maastricht, The Netherlands. To exclude possible hybridization to RNA transcripts, cells were treated with 10 ng/ml ribonuclease A (Qiagen) in a control experiment.

DNA FISH. Fluorescence *in situ* hybridisation (FISH) was performed as described earlier.[12,27] Briefly, cells were fixed in 70% ethanol, incubated with 0.01% pepsin (800–1200 U/mg protein from porcine stomach mucosa; Sigma) in 0.01N HCl and post-fixed in 1% formaldehyde in PBS. Probe and target DNA were denatured simultaneously for 3 min at 80°C prior to hybridization overnight at 37°C in a humid chamber. After hybridization, the preparations were washed stringently. Biotin-labeled probe was detected using FITC-conjugated-avidine (Vector Laboratories, Burlingame, CA), biotin-conjugated goat-anti-avidin

(Vector) and again FITC-conjugated-avidin. In cases where two hybridization probes were used simultaneously, biotin-labeled probes were detected as described above. The digoxigenin-labeled probe was detected using mouse-anti-digoxigenin, TRITC-conjugated rabbit-anti-mouse and finally TRITC-conjugated swine-anti-rabbit (all from Dako, Glostrup, Denmark). Slides were mounted in Vectashield (Vector) containing 4′,6-diamidino-2-phenylindole (DAPI; Sigma).

RNA FISH. The HPV16 RNA specific FISH was performed on CytoRichRed-fixed, paraffin-embedded slides of the different cell lines according to Smedts *et al.*[28] or on 70% ethanol suspensions additionally fixed in CytoRichRed. In contrast to DNA FISH, cells were rehydrated in an ethanol series using RNAse block (Biogenex) in the 50% ethanol and demineralized water solutions, digested with proteinase K (DAKO PNA ISH detection kit) for 20 min at RT and hybridized with denatured digoxigenin-labeled HPV16 DNA probes. Cells were not denatured to allow hybridization to viral RNA and to prevent hybridization to viral DNA. After overnight hybridization, the slides were processed according to the FISH protocol described above. As a negative control, slides were treated with RNAse.

Images were acquired using a Leica DMRXA microscope (Leica, Wetzlar, Germany) equipped with optical filters for DAPI, fluorescein and TRITC and a 63× Plan Apo (NA 1.32) objective. The microscope was connected to a digital black and white CCD camera (Metasystems Image Pro System, Sandhausen, Germany) for image recording. Staining patterns were scored as described earlier.[29]

Metaphase spreads. Metaphase spreads were made as described previously,[30] with minor adjustments. Briefly, cells were cultured until ~50% confluency. Medium was then replaced by medium containing 0.1–0.5 μg/ml colcemid (Sigma) and 0–0.01 μg/ml ethidium bromide and incubated for 2–4 hr at 37°C. Optimal conditions varied per cell line. After incubation, cells were trypsinized and subsequently treated with 0.075 M KCl for 10 min at 37°C. Cells were washed twice and fixed in methanol/acetic acid (3:1, v/v). FISH probes were used for hybridization as outlined above, with minor adjustments. Slides were only incubated for 8 min with 0.01% pepsin (800–1200 U/mg protein from porcine stomach mucosa; Sigma) in 0.01N HCl at 37°C. After washing, slides were dehydrated in an ascending ethanol series and air dried. Slides were then baked for 10 min at 56°C. Postfixation was performed in 4% formaldehyde in PBS for 10 min at RT. After postfixation, the protocol was followed as described above.

Amplification of papillomavirus oncogene transcripts (APOT-PCR). HPV oncogene transcripts were amplified as described before.[10,27] Briefly, reverse transcription was performed using 25 μM oligo-$(dT)_{17}$ primer coupled to a linker sequence $(dT)_{17}$-p3, 10 mM dNTPs each, 0.1 M DTT, 5× RT-buffer and SuperScript reverse transcriptase (Invitrogen, Karlsruhe, Germany). Quality of cDNA was determined by a standard *GAPDH* gene PCR. First-strand cDNAs containing viral oncogene sequences were subsequently amplified with semi-nested PCR using HPV-E7 specific 5′-primers and oligo(dT) and adaptor primers (3′). PCR products were separated on a 1.2% agarose gel. All bands were cut out, purified (QIAGEN Gel extraction kit, QIAGEN, Hilden, Germany) and sequenced (GATC Biotech, Konstanz, Germany). Sequence results were analyzed using the BLASTN program[31] and further mapped using map viewer, both provided by the National Center for Biotechnology Information (NCBI).[25]

Detection of integrated papillomavirus sequences (DIPS-PCR). Integrated papillomavirus sequences were detected using the Detection of Integrated Papillomavirus Sequences-PCR (DIPS-PCR) assay, as described earlier.[27,32] Briefly, genomic DNA was digested using the Sau3AI restriction enzyme and an enzyme-specific adapter was ligated to the restriction-digested DNA using T4 DNA ligase (Roche Diagnostics, Mannheim, Germany). Linear PCR was performed using five HPV16 specific forward primers in independent setups. All independent PCRs were followed by individual exponential PCRs using further virus-specific forward primers and the AP1 reverse primer. PCR products were separated on a 1.2% agarose gel and products of interest were excised and subsequently sequenced (GATC Biotech). Sequence results were analyzed using the BLASTN program[31] and further mapped using map viewer, both provided by the NCBI.[25]

mRNA expression of HPV16 E2, E6 and E7 and human EGFR

RNA was reverse transcribed using the iScript cDNA Synthesis Kit (BioRad Laboratories, Hercules, CA). Real-time PCR reactions were performed using SensiMix SYBR & Fluorescein (GC Biotech, Alphen a/d Rijn, The Netherlands). The detection of the housekeeping gene *hypoxanthine phosphoribosyltransferase* (*HPRT*) was used for normalization of mRNA levels. Primer sequences for *HPRT* were kindly provided by Prof. Dr. L. Hofland from Erasmus Medical Centre, Rotterdam, The Netherlands. The following primers, synthesized by Biolegio BV, were used:

Target	Primer	Sequence	Ref
HPV16 E2	Forward	5′-TGATAGTACAGACCTACGTGACC ATATAGA-3′	
	Reverse	5′-ATTACAAGGCCAGAGAAATGGG-3′	
HPV16 E6	Forward	5′-CAGTTATGCACAGAGCTGCAA-3′	33
	Reverse	5′-ATGACTTTGCTTTTCGGGATT-3′	
HPV16 E7	Forward	5′-AGAGGAGGAGGATGAAATA GATGGT-3′	
	Reverse	5′-CAATATTGTAACCTTTTGTTGCA AGTG-3′	
EGFR	Forward	5′-CCAAGGGAGTTTGTGGAGAA-3′	
	Reverse	5′-CTTCCAGACCAGGGTGTTGT-3′	
HPRT	Forward	5′-CACTGGCAAAACAATGCAGACT-3′	34
	Reverse	5′-GTCTGGCTTATATCCAACACTTCGT-3′	

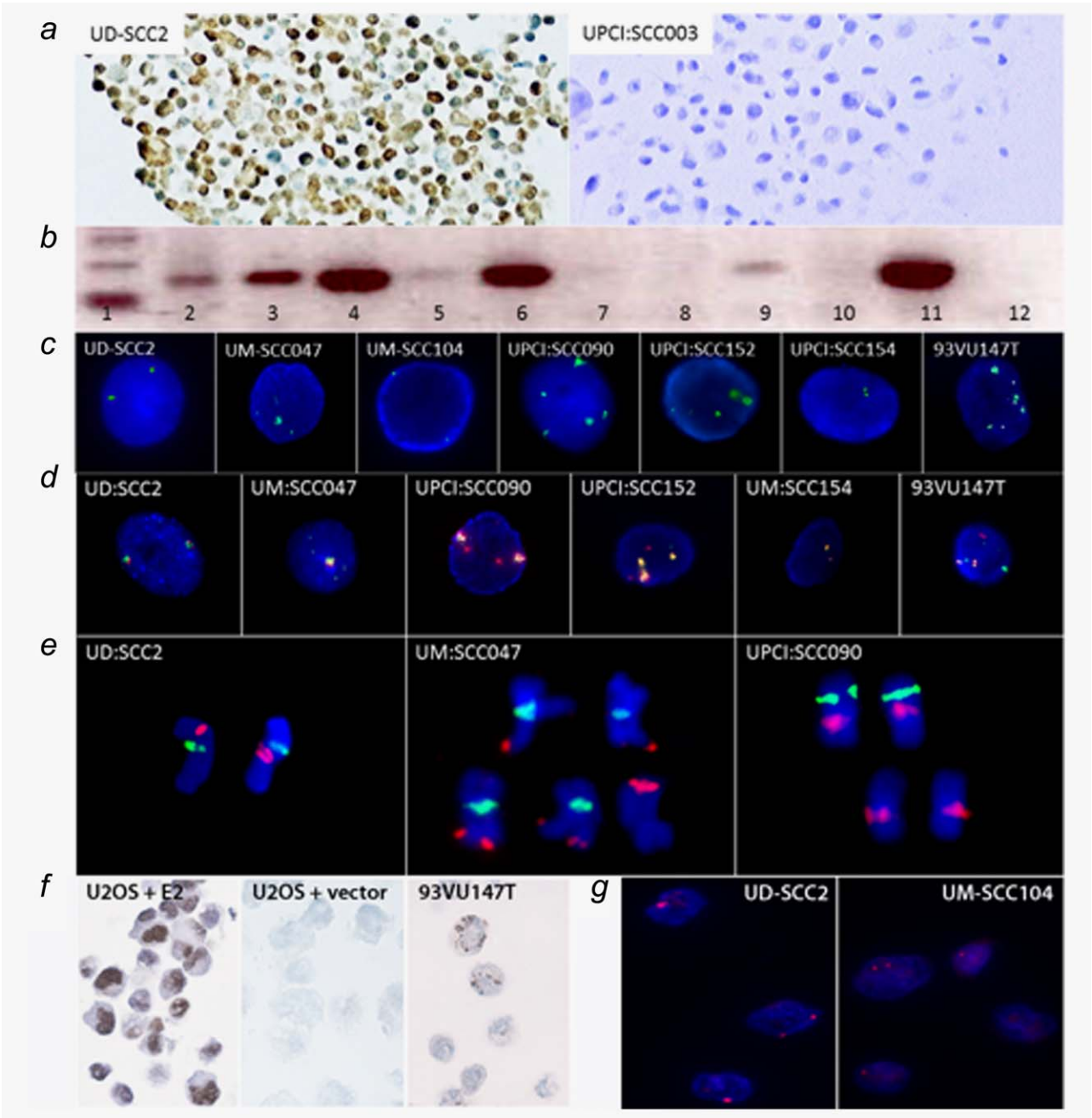

Figure 1. Representative examples of $p16^{INK4A}$ staining in cell lines UD-SCC-2 (HPV16 positive) and UPCI:SCC003 (HPV-negative). HPV16-specific PCR. Lane 1 shows the 100, 200, and 300 bp fragments of a 100 bp ladder for fragment size determination, lane 2–12 show the results of the HPV16 specific PCR. Lane 2: UD-SCC-2; lane 3: UM-SCC-047; lane 4: UPCI:SCC090; lane 5: UM-SCC-104; lane 6: UPCI:SCC152; lane 7: UPCI:SCC154; lane 8: U2OS cell line with the empty pJ4Ω-vector as negative control; lane 9: 93VU147T; lane 10: HeLa (HPV18 cervix carcinoma cell line); lane 11: CaSki (HPV16 positive cervix carcinoma cell line); lane 12: water. HPV16 FISH staining pattern in the seven cell lines. HPV16 was detected using a FITC-labeled probe (green) and cell nuclei are stained with DAPI (blue). Colocalization of FITC-labelled HPV16 probes (green) with TRITC-labeled BAC clones (red) on interphase nuclei of UD-SCC-2 (BAC clone RP11–212B22), UM-SCC-047 (BAC clone RP11–373I6), UPCI:SCC090 and UPCI:SCC152 (BAC clone RP11–23B15 for both), UPCI:SCC154 (BAC clone RP11-10J13) and 93VU147T (BAC clones RP11–1331M22 and RP11–365D23, respectively). Colocalisation of HPV16 probes with probes for CEPX (green), CEP3 (green) or CEP9 (red) on metaphase spreads of UD-SCC-2, UM-SCC-047 and UPCI:SCC090, respectively. Images of HPV16-E2 protein expression in U2OS cells with E2 containing pJ4Ω-vector (positive control; left), U2OS cells with empty pJ4Ω-vector (negative control; middle), and 93VU147T cell line (right), showing diffuse nuclear immunostaining, no staining and numerous immunostained nuclear foci, respectively. Counterstaining was done with Haematoxylin. Images of HPV16 RNA FISH on UD-SCC-2 (left) and UM-SCC-104 (right) cell lines showing variable numbers of transcriptionally active integration sites (red signals) in DAPI counterstained nuclei (blue).

Table 2. Results obtained in HPV-positive cell lines for the analysis of viral load, FISH, cohybridization of HPV16 and BAC-probes containing human DNA sequences detected by APOT- and/or DIPS-PCR, aneuploidy status and the expression of the viral genes

Cell line	Viral Load	HPV16 FISH	BAC-clone[1]	Colocalization[2]	Additional chromosomal locations[3]	Aneuploidy[4]	Viral gene expression		
	HPV16 copies/ β-globin copy	Signals/ nucleus				CEP1:CEP7	*E2*	*E6*	*E7*
UD-SCC-2	22	2	RP11–212B22	yes, 2/2		3:3	5,897	6,364	22,717
UM-SCC-047	15	5	RP11–373I6	yes, 5/5		4:5	1,505	2,514	6,899
UM-SCC-104	1	1–4		ND	not detected	3:4	0,555	3,340	29,464
UPCI:SCC090	739	6	RP11–23B15	yes, 2/6	2 signals on chromosome 32 signals on chromosome 6	6:3	1,526	4,408	11,472
UPCI:SCC152	210	6	RP11–23B15	yes, 2/6	4 additional signals, not yet identified	6:3	0,624	6,021	14,390
UPCI:SCC154	1	2	RP11-10J13	yes, 2/2		2:2	0,000	0,616	2,085
93VU147T	58	7	RP11–1331M22	yes, 3/7	4 additional signals, not yet identified	4:3	5,134	1,165	4,395

[1]Indicates the BAC-probe that was used for the cohybridization experiments.
[2]Indicates whether the BAC-probe colocalized with the HPV-16 probe (number of colocalizing BAC-signals/total HPV-signals per nucleus).
[3]Additional information for HPV integration obtained from HPV16-specific FISH analysis on metaphase spreads of the cell lines.
[4]Aneusomies for chromosomes 1 and 7 in the dominant cell population.

Immunohistochemistry for HPV16 E2

CytoRichRed-fixed (3 μM), paraffin-embedded slides were used for immunohistochemistry. The slides were deparaffinized using xylol, rehydrated in a descending ethanol series and pretreated with citrate buffer pH 6.1 (DAKO, EnVision FLEX Target Retrieval Solution, Low pH) for 10 min at 97°C. Primary mouse monoclonal anti-HPV16-E2 antibody (Clone TVG 261; 1:100, Merck Millipore Corporation, Amsterdam, The Netherlands) was added to the slides and incubated for 1 hr at RT, followed by incubation with FLEX+ Mouse LINKER (DAKO) for 20 min at RT and EnVision FLEX/HRP (DAKO) for 30 min at RT. HRP was visualized using DAB+ Chromogen (DAKO) substrate. Between all of the incubation steps, the slides were washed with wash buffer (DAKO). Finally, slides were counterstained with hematoxylin, dehydrated and mounted in Vectashield (Vector). Images were recorded in the brightfield mode using the microscope described above.

Results

Active HPV16 infection is present in all cell lines

All cell lines have been tested for active HPV16 infection using the algorithm suggested previously.[4] AgarCyto blocks of the cell lines showed overexpression of the CDK-inhibitor $p16^{INK4A}$ using immunocytochemistry, which is routinely used as a surrogate marker for HPV infection (see Fig. 1*a*). Furthermore, the presence of HPV16 DNA has been shown by PCR, first using the consensus primers GP5+/6+ and subsequently by using type-specific primers for HPV16 and 18 (see Fig. 1*b*). RT-PCR analysis of the viral oncogenes *E6* and *E7* showed viral gene expression in all cell lines (see below).

Viral load

HPV16 load in all cell lines was estimated using PCR and was expressed as the number of HPV16 copies per *β-globin* copy. Viral load varied from 1 (UM-SCC-104) up to 739 (UPCI:SCC090) HPV16 copies per human *β-globin* gene copy (see Table 2).

DNA FISH integration analysis

All cell lines were tested for the presence of HPV16 DNA using FISH on 70% ethanol suspensions and they all showed a reproducible punctate nuclear signal, which indicates viral integration. Each cell line showed a specific number of FISH signals per nucleus, ranging from 2 (UD-SCC-2 and UPCI:SCC154) to 7 (93VU147T) (Fig. 1*c*). UPCI:SCC090 and −152, derived from the same patient, showed identical spot numbers. UM-SCC-104, however, showed a variable number of signals per nucleus, ranging from 1 to 4 (Table 2). Notably, cell lines with a high viral load exhibited a higher number and/or more intense FISH signals (see Fig. 1*c* and Table 2) and showed stronger HPV16-specific PCR bands on agarose gel (see Fig. 1*b*). Possible hybridization to RNA transcripts was excluded by treating the cells with RNAse in a control experiment.

Table 3. Identified HPV16 integration sites in HPV-positive HNSCC cell lines using DIPS- and APOT-PCR

	APOT-PCR							DIPS-PCR						
Cell line	HPV stat.[1]	Transcr. Type[2]	mRNA splice structure[3]	Map	Accept. Site[4]	Database comparison[5]	Fragile site[6] (distance)	HPV stat[1]	Viral disruption[7] (nt)	Viral insertion[8] (nt)	Map	Integr. Locus[9]	Database comparison[5]	Fragile site[6]
UD-SCC-2	I	A	HPV:880^HSC_X:(-)96396691	Xq21.33	Exon 21 coding	DIAPH2 NC_000023.10	FRAXC Xq22.1 (~5 Mb)	I	3105 (E2)	X:(−)96369882	Xq21.33	Exon 20 coding	DIAPH2 NC_000023.10	FRAXC Xq22.1 (~5 Mb)
UM-SCC-047	I	A	HPV:880^HSC_3:(+)189604183	3q28	Exon 7 coding	TP63 NC_000003.11	FRA3C 3q27 (~5,5 Mb)	I	1299 (E1)	3:(+)189567310	3q28	Intron 4 coding	TP63 NC_000003.11	FRA3C 3q27 (~5,5 Mb)
UM-SCC-104	E							E						
UPCI: SCC090	I + E	A	HPV:880^HSC_9:(−)100675840	9q22.33	Exon 4 coding	C9orf156 NC_000009.11	FRA9D 9q22.1 (~9 Mb)	I + E	2099 (E1)	9:(−)100676842	9q22.33	Intron 2 coding	C9orf156 NC_000009.11	FRA9D9q22.1 (~9 Mb)
UPCI: SCC152	I + E	A	HPV:880^HSC_9:(−)100675840	9q22.33	Exon 4 coding	C9orf156 NC_000009.11	FRA9D9q22.1 (~9 Mb)	I+E	2099 (E1)	9:(−)100676842	9q22.33	Intron 2 coding	C9orf156 NC_000009.11	FRA9D 9q22.1 (~9 Mb)
UPCI: SCC154	I	A	HPV:880^HSC_21:(−)16635988	21q11.2	Inter	NC_000021.8		I	2067 (E1)	21:(−)16427783	21q11.2	Intron 1 opp.	NRIPI NC_000021.8	
93VU147T	I+E	A	HPV:880^HSC_17:(+)36430708	17q12	Inter	NC_000017.10	FRA17B 17q23.1 (~21,5 Mb)	I + E	1067 (E1)	17:(+)36423208	17q12		Inter NC_000017.10	FRA17B 17q23.1 (~ 21,5 Mb)

[1]HPV stat indicates (E)pisomal or (I)ntegrated status of HPV as detected by used method.
[2]Transcript type, A=splicing directly to the human sequence.
[3]Splice structure from viral donor site 880 (HPV880) to viral acceptor site (^HPVnucleotide) and/or human genome as indicated (^HSC_chromosome number:(strand)nucleotide). HSC = homo sapiens chromosome.
[4]Acceptor site indicates whether splicing has taken place to an intron, exon or intergenic region (inter) and whether in the coding or opposite (opp) strand. The intron or exon number is also indicated. All Data refer to GRCh37.p5 Primary Assembly. Numbering of HPV16 sequence according to GenBank Accession number NC_001526.
[5]GenBank gene name and accession number of corresponding whole chromosome sequence.
[6]Fragile sites according to NCBI Map View, for distances ≥5 Mb the approximate distance to viral insertion site is indicated.
[7]Viral disruption (nt) indicates the last nucleotide of HPV sequence.
[8]Viral insertion (nt) indicates the first nucleotide of the insertion site for the human genome, where (+) indicates forward and (−) indicates reverse strand.
[9]Integration locus indicates whether integration has taken place in an intron (int), exon (ex) or intergenic region (inter) and whether in the coding or opposite (opp) strand. The intron or exon number is also indicated.

Identification of HPV16 integration sites by PCR

APOT-PCR, a PCR-based method that can amplify both viral-human fusion transcripts as well as episome-derived viral transcript, was used to identify the site of viral integration in the cellular genome. A single integration site was identified in five cell lines (UM-SCC-047, UPCI:SCC090, UPCI:SCC152, UPCI:SCC154 and 93VU147T; see Table 3). Sequencing analysis of the obtained viral-human fusion transcripts revealed viral integration in 3 genes and in 2 intergenic regions. The protein-coding regions identified were *DIAPH2*, exon 21 (UD-SCC-2), *TP63* exon 7 (3q28, UM-SCC-047) and *NAP1* exon 4 (9q22.33, UPCISCC:090 and UPCI:SCC152; both derived from two subsequently diagnosed recurrent tumors from the same patient). The intergenic regions identified were located on chromosomes 17q12 (93VU147T) and 21q11.2 (UPCI:SCC154).

All fusion transcripts detected by APOT-PCR showed type A splicing as described by Klaes *et al.*[10] from viral nucleotide 880 directly into the human sequence in sense orientation with the identified gene. Interestingly, only episomal transcripts could be identified in the UM-SCC-104 cell line, suggesting the presence of complete episomes, either integrated or extrachromosomal. DIPS-PCR was performed to verify the identified integration sites and to search for possible viral-human fusion products in the cell line where no fusion transcript could be identified using APOT-PCR (UM-SCC-104). No fusion product could be amplified in this cell line, although the presence of episomal viral copies was confirmed. In the remaining cell lines the integration sequences identified using APOT-PCR were confirmed by DIPS-PCR. DIPS-PCR identified the integration site in the UPCI:SCC154 cell line to be located within the *NRIP1* gene. Identified integration sites are summarized in Table 3.

To confirm that the identified human sequences were localized adjacent to the viral genome, double-target FISH analysis was performed using both the HPV16 probe and BAC-probes complementary to the putative integration sequence (see Fig. 1*d*). BAC-probes were shown to colocalize with all HPV16 signals in two cell lines (UM-SCC-047 and UPCI:SCC154). In three additional cell lines, HPV16 signals were also detected without colocalization with the BAC-probe (UPCI:SCC090, UPCI:SCC152 and 93VU147T).

HPV mapping on metaphase preparations

For the cell lines in which the integration loci did not colocalize to a BAC-probe (UM-SCC-104, UPCI:SCC090 and 93VU147T), HPV16 FISH analysis in combination with karyotyping based on inverted DAPI staining was performed on metaphase preparations. All data are summarized in Table 2. In the UPCI:SCC090 cell line additional integration events were mapped to chromosomes 3 and 6, which is in agreement with published data.[35,36] Interestingly, in the metaphase preparations of the UM-SCC-104 cell line, metaphase chromosomes did not show HPV16 FISH signals, whereas interphase cells, also present in the preparation, did show a nuclear FISH staining pattern similar to the staining on 70% ethanol suspensions (see Fig. 1*c*). This was shown in repeated experiments with different observers (JvLA, E-JS and NO). Although this might be a sensitivity issue, another explanation might be that the virus is extrachromosomal, which is supported by the detection of only episomal transcripts by APOT- and DIPS-PCR (see above).

Integration events and ploidy status

To determine whether multiple colocalizing FISH-signals indicated duplication or translocation of the involved chromosome, double-target FISH was performed on metaphase preparations of the cell lines, using both a CEP-probe as well as an HPV probe. This showed that integration can be followed by deletion of the sister chromosome and duplication (UD-SCC-2) or multiplication (UM-SCC-047) of the chromosome containing HPV integration, with all respective chromosomes showing signals for both the CEP-probe as well as the HPV16 probe. Duplication of chromosomes with concurrent duplication of the sister chromosome was also seen (UPCI:SCC090, UPCI:SCC152), shown by the presence of chromosomes containing only a signal for the CEP-probe as well as chromosomes containing signals for both CEP- and HPV16 probes. Lastly, duplication could also be accompanied by translocation of a small portion of the involved chromosome to a different chromosome (UM-SCC-047).

The detected multiplication of chromosomes is in line with the ploidy status of the different cell lines, which in six of the seven cell lines showed copy number variations for chromosomes 1 and 7, a hallmark for chromosomal instability and aneusomy[8] (Table 2).

Gene expression of HPV16 E2, E6 and E7 and human EGFR

To determine whether integration affects the expression of the viral genes, the expression levels of the viral genes *E2*, *E6* and *E7* were determined using RT-PCR (see Fig. 2). Expression of the viral gene E2, which is known to regulate gene transcription of the oncogenes *E6* and *E7,* was present at variable levels in six of the seven cell lines. To verify the presence of HPV16-E2 protein expression, we carried out immunohistochemistry on tissue sections of five CytoRichRed fixed and paraffin embedded cell lines, a positive control (U2OS cell line transfected with E2) and a negative control (U2OS cell line transfected with empty pJ4Ω-vector; Fig. 1*f*). U2OS E2 cells showed a strong diffuse nuclear immunostaining in all cells. U2OS vector cells and the UM-SCC104 cell line were negative and the cell lines UPCI:SCC090, 93VU147T, UD-SCC-2, UM-SCC47 showed E2 positive foci in the nuclei at a frequency of 43, 9, 2 and 0.5%, respectively. mRNA expression of the viral oncogenes *E6* and *E7* could be detected in all cell lines at variable levels, but no correlation could be found with the levels of *E2* mRNA expression.

No correlation was found between the number of FISH HPV16 signals, viral load and viral mRNA gene expression.

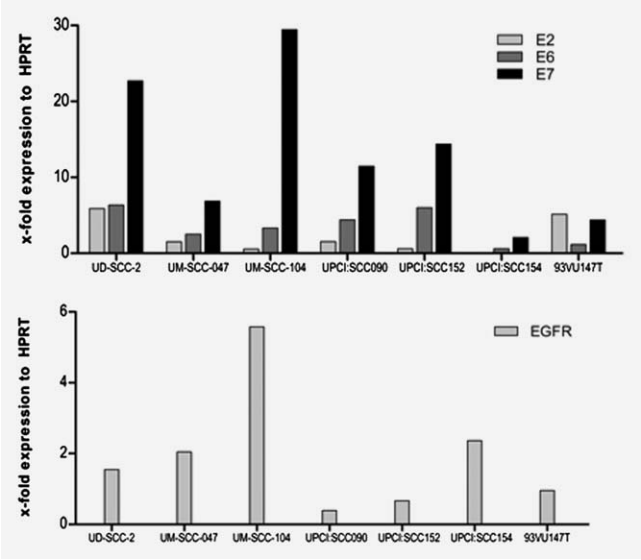

Figure 2. Expression of viral genes *E2*, *E6,* and *E7* for each of the seven cell lines. Expression levels are displayed as x-fold change as compared with the expression of the housekeeping gene *HPRT*. Expression of *EGFR* for each of the seven cell lines. Expression levels are displayed as x-fold change as compared to the expression of the housekeeping gene *HPRT*.

To verify if all DNA-FISH detected HPV16 integration sites are transcriptionally active, we performed RNA FISH (see Supporting Information Table S1). These data showed that there is a variation of transcriptionally active sites within different cells of each cell line ranging from the maximum number of viral integration signals up to zero. To ensure that this variation was not the result of incomplete cells due to the cutting of tissue sections, we also performed RNA FISH on 70% ethanol suspensions leading to comparable results (data not shown).

In addition, the level of *EGFR* expression was examined for each of the seven cell lines. This showed variable expression of 0.4 (UPCI:SCC090) up to 5.6-fold (UM-SCC-104) expression to *HPRT*. As the median *EGFR* expression in 61 primary HPV-associated HNSCC is 0.3 fold to *HPRT* (range 0.001–18.6-fold to *HPRT,* unpublished results), this indicates increased expression of *EGFR* in all cell lines.

Discussion

HR-HPV infection is a well-established risk factor contributing to the development of HNSCC, particularly OSCC. HPV-positive tumors have different clinical and pathobiological characteristics, including a better prognosis as compared to HPV-negative tumors.[4] It is still under debate, which factors, in addition to the presence of HPV DNA and the resulting viral gene expression in the host cell, are contributing to tumor development and progression. For example, integration of the viral DNA into the host genome and the resulting disruption of invaded genes might play an important role in the process of HPV carcinogenesis, as seen in HPV-associated cervical cancer. In the case of HNSCC, few studies have addressed this highly relevant issue.[26,36–39]

Since *in vitro* testing is still an important step in the development of new therapeutic options, it is imperative to be able to study well-established cell line models for HPV-positive HNSCC. In the underlying study, HPV16-associated parameters, such as viral load and integration, have been assessed in seven established HNSCC cell lines, shown to be HPV-induced by $p16^{INK4A}$ immunostaining and HPV-type-specific PCR.

Integration of HPV DNA was detected in six of the seven cell lines using three independent methods, *i.e.* APOT- and DIPS-PCR and FISH, which all gave concurrent results with respect to the integration locus. Furthermore, for three cell lines (UD-SCC-2, UM-SCC-47 and UPCI:SCC090) our results confirmed previously reported integration sites.[35,36] Two cell lines that were derived from the same patient (UPCI:SCC090 and UPCI:SCC152), showed identical integration sites despite the fact that they were established from biopsies taken from different locations and at different time points, indicating clonal expansion of the tumor. One cell line (UM-SCC-104) did not show integration, but rather the presence of extrachromosomal HPV DNA, as assessed by APOT- and DIPS-PCR. This is in contrast to a recent study by Akagi *et al.*, suggesting viral integration in this cell line.[36] However, in our opinion their presented FISH and Northern blotting data on UM-SCC-104 did not provide sufficient evidence for viral integration. We were unable to detect the integrated virus DNA on metaphase chromosomes of the cell line and it is very unlikely that we missed this integration site by our DIPS- and APOT-PCR assay in the here presented study. Maybe the detected deletion in HPV16-E2 by Akagi *et al.* using whole genome sequencing is present in episomal DNA or alternatively viral integration or loss of the integration site in UM-SCC-104 could be a result of culturing.[36]

We detected viral loads varying from 1 up to 739 HPV16 copies per β-globin gene copy. In contrast to results obtained from cervical malignancies,[40] viral load did not seem to be correlated to integration status. This can be concluded from the two cell lines showing a viral load of 1 HPV DNA copy per β-globin copy, one of which showed HPV DNA integration and the other showed only episomal HPV.

Cell lines with a higher viral load did exhibit strong punctate FISH signals, indicating that the HPV genome may be present in integrated tandem repeats. This assumption is supported by the finding that these strong signals are not derived from RNA transcripts present at these loci, since RNAse treatment before the DNA FISH analysis did not lead to a substantial decrease in signal intensity (data not shown). Moreover, the cell lines showed two up to seven HPV integration sites by FISH, whereas in primary tumors generally only one signal per nucleus is detected.[8] To determine whether this is due to either multiplication of the integration locus or a result of multiple independent integration events,

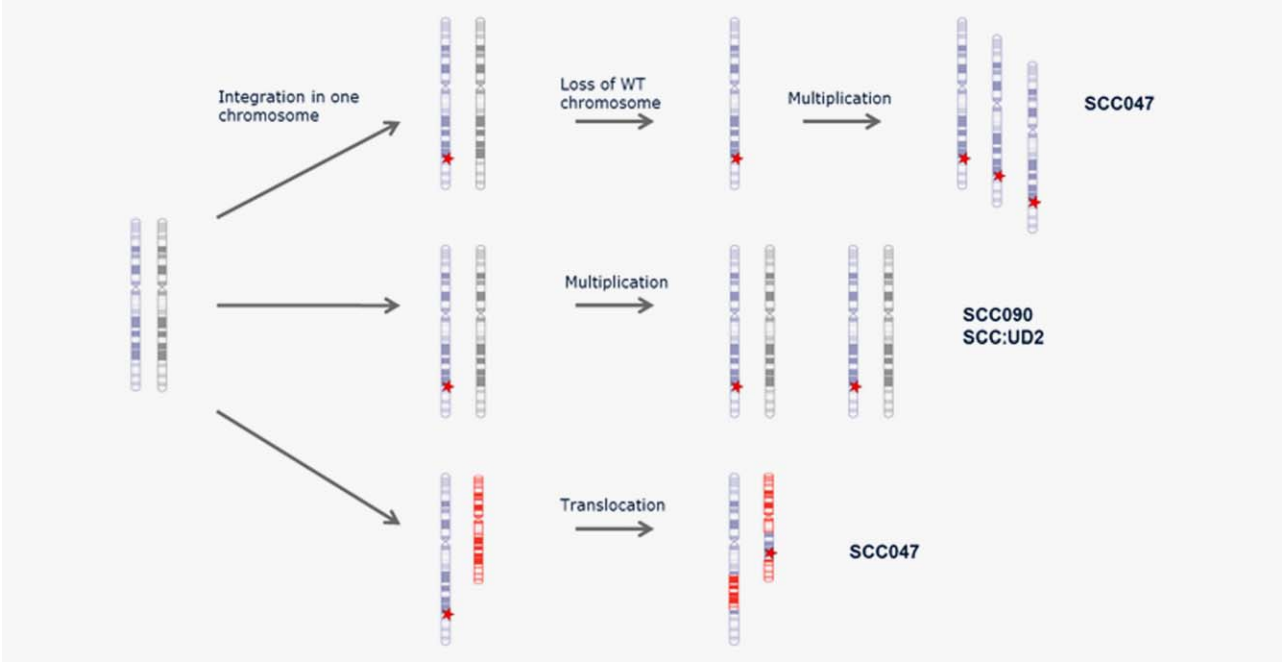

Figure 3. Schematic representation of the possible multiplication and translocation events in the cell lines. High-risk human papillomavirus (HPV) infection is a well-established risk factor for head and HNSCC development. It is still unclear, however, whether viral DNA integration into the host genome plays an important role in HPV carcinogenesis in HNSCC. In this study, seven HPV16-positive HNSCC cell lines showed integrated and/or episomal viral DNA that is transcriptionally active. Both viral load and expression of several viral early genes were variable. Because the cell lines also feature EGFR overexpression and aneusomy, which are parameters of poor prognosis, they may represent suitable model systems for the development of new antiviral therapies.

cohybridization of HPV16 probes with a BAC-probe complementary to the identified integration sequences was performed. In the cell lines UD-SCC-2, UM-SCC-047 and UPCI:SCC154 all HPV16 signals were shown to colocalize with the BAC-probe, while in UPCI:SCC090, UPCI:SCC152 and 93VU147T the BAC-probe colocalized with part of the HPV16 FISH signals. The presence of more than one colocalizing signal indicates multiplication of the integration locus. Multiplication of an existing integration site was furthermore shown by cohybridization of the HPV-probe with CEP-probes for the corresponding chromosome. For the UD-SCC-2 cell line, derived from a male patient, the two HPV16 FISH signals were located on two different CEPX-containing chromosomes, indicating that a duplication event has occurred. In the UPCI:SCC090 four chromosome copies containing CEP9 were detected, of which two harboured HPV16 signals, indicating duplication of both copies of chromosome 9. In the UM-SCC-047 cell line, five HPV16 signals were detected on five separate chromosomes, of which four also contained CEP3, indicating multiplication of the initial integration site. The fifth chromosome contained very strong HPV- and BAC-signals, but no CEP3 signal (see Fig. 1*e*), which might indicate that this chromosome evolved by a different mechanism, for example involving both translocation of part of chromosome 3 and amplification of the integration site. Figure 3 provides a schematic representation of the multiplication and translocation events identified in the HNSCC cell lines indicated. This finding further supports the results of Akagi *et al.* that show that HPV integrants may promote genomic instability.[36]

Besides HPV16 signals colocalizing with the BAC-probe in UPCI:SCC090, UPCI:SCC152 and 93VU147T cell lines, additional HPV16 signals were detected. The non-colocalizing HPV signals might indicate multiple independent integration events, which were not detected by APOT- or DIPS-PCR. A possible explanation for the fact that the APOT-PCR assay is unable to detect all the different integration sequences may be that (several of) these sequences are not actively transcribed and therefore are not clinically relevant. However, the inability of the DIPS-PCR assay to detect these integrated sequences may come from an alternative integration mechanism that is not detected by our PCR, which is based on *E1* and *E2* HPV sequences. Using DIPS-PCR with additional primers covering the entire HPV genome, Li *et al.*[41] described a mechanism for HPV16 integration in exfoliated cervical cells based on disruption of the *L1* or *L2* gene. These authors indicated that integration at these viral sites would normally not result in progression to (pre)malignant lesions. It is therefore likely that such integration events have occurred in our cell lines, before or after the clinically relevant integration event took place.

From studies in cervical cancer it is known that viral load does not necessarily correlate to expression levels of *E6* and *E7*.[42] Similarly, in the HNSCC cell lines, as well as in primary

HNSCC, the variation in viral load was not reflected in the expression of the viral genes *E2*, *E6* and *E7*. Furthermore, the current concept of cervical carcinogenesis suggests that HPV integration leads to disruption of the viral genome in the *E1* or *E2* open reading frame (ORF), followed by loss of the *E2* inhibitory gene function on *E6* and *E7* expression. Subsequently expression of both oncogenes is thought to be enhanced.[33,34,43] However, in the different HNSCC cell lines, such a correlation could not be found. *E2* mRNA and protein levels were highly variable in UD-SCC-2, UM-SCC-47, UPCI:SCC090, UPCI:SCC152 and 93VU147T, even though integration was identified. A recent publication suggests that HPV integration without concurrent loss of the *E2* gene can also occur in HNSCC resulting in viral concatenates in the human genome.[37] The high viral load in combination with a limited number of strong FISH signals indicates that integration of such stretches of multiple HPV-copies could have occurred in our cell lines as well. *E6* and *E7* mRNA levels were equally variable in all cell lines and no correlation was seen with the expression levels of *E2*. This is in agreement with the results obtained in primary HNSCC, in which the expression levels of *E2*, *E6* and *E7* mRNA transcripts were highly variable and did not show correlation to the physical status of the virus.[8,27]

In conclusion, we have characterized seven established HPV16-positive HNSCC cell lines, which showed integrated and/or episomal viral DNA that is transcriptionally active. However, viral E2, E6 and E7 gene expression proved to be independent of viral load and the number of viral integration sites, suggesting that integration does not affect viral gene expression. The analyzed cell lines, furthermore, exhibit characteristics of primary HPV-positive OSCC with a poor prognosis, such as *EGFR* overexpression and aneusomy,[8,44,45] although it cannot be ruled out completely that molecular changes may have accumulated due to cell culturing. We believe that these cell lines represent suitable model systems of HPV-positive HNSCC that respond poorly to current treatment modalities and that they may be beneficial in future studies for the analysis of new treatment options.

References

1. Klussmann JP, Weissenborn SJ, Wieland U, et al. Prevalence, distribution, and viral load of human papillomavirus 16 DNA in tonsillar carcinomas. *Cancer* 2001;92:2875–84.
2. D'Souza G, Kreimer AR, Viscidi R, et al. Case-control study of human papillomavirus and oropharyngeal cancer. *N Engl J Med* 2007;356:1944–56.
3. Ragin CCR, Modugno F, Gollin SM. The epidemiology and risk factors of head and neck cancer: a focus on human papillomavirus. *J Dent Res* 2007;86:104–14.
4. Olthof NC, Straetmans JM, Snoeck R, Ramaekers FC, Kremer B, Speel EJ. Next-generation treatment strategies for human papillomavirus-related head and neck squamous cell carcinoma: where do we go? *Rev Med Virol* 2011;22:88–105.
5. Lassen P, Eriksen JG, Hamilton-Dutoit S, et al. HPV-associated p16-expression and response to hypoxic modification of radiotherapy in head and neck cancer. *Radiother Oncol* 2010;94:30–5.
6. Maxwell JH, Kumar B, Feng FY, et al. Tobacco use in human papillomavirus-positive advanced oropharynx cancer patients related to increased risk of distant metastases and tumor recurrence. *Clin Cancer Res* 2010;16:1226–35.
7. Ang KK, Harris J, Wheeler R, et al. Human papillomavirus and survival of patients with oropharyngeal cancer. *N Engl J Med* 2010;363:24–35.
8. Mooren JJ, Kremer B, Claessen SMH, et al. Chromosome stability in tonsillar squamous cell carcinoma is associated with HPV16 integration and indicates a favorable prognosis. *Int J Cancer* 2013;132:1781–9.
9. Theelen W, Speel EJM, Herfs M, et al. Increase in viral load, viral integration, and gain of telomerase genes during uterine cervical carcinogenesis can be simultaneously assessed by the HPV 16/18 MLPA-assay. *Am J Pathol* 2010;177:2022–33.
10. Klaes R, Woerner SM, Ridder R, et al. Detection of high-risk cervical intraepithelial neoplasia and cervical cancer by amplification of transcripts derived from integrated papillomavirus oncogenes. *Cancer Res* 1999;59:6132–6.
11. Saunier M, Monnier-Benoit S, Mauny F, et al. Analysis of human papillomavirus type 16 (HPV16) DNA load and physical state for identification of HPV16-infected women with high-grade lesions or cervical carcinoma. *J Clin Microbiol* 2008;46:3678–85.
12. Hafkamp HC, Speel EJ, Haesevoets A, et al. A subset of head and neck squamous cell carcinomas exhibits integration of HPV 16/18 DNA and overexpression of p16INK4A and p53 in the absence of mutations in p53 exons 5–8. *Int J Cancer* 2003;107:394–400.
13. Mellin H, Dahlgren L, Munck-Wikland E, et al. Human papillomavirus type 16 is episomal and a high viral load may be correlated to better prognosis in tonsillar cancer. *Int J Cancer* 2002;102:152–8.
14. Koskinen WJ, Chen RW, Leivo I, et al. Prevalence and physical status of human papillomavirus in squamous cell carcinomas of the head and neck. *Int J Cancer* 2003;107:401–6.
15. Begum S, Cao D, Gillison M, et al. Tissue distribution of human papillomavirus 16 DNA integration in patients with tonsillar carcinoma. *Clin Cancer Res* 2005;11:5694–9.
16. Chang YE, Pena L, Sen GC, et al. Long-term effect of interferon on keratinocytes that maintain human papillomavirus type 31. *J Virol* 2002;76:8864–74.
17. Herdman MT, Pett MR, Roberts I, et al. Interferon-beta treatment of cervical keratinocytes naturally infected with human papillomavirus 16 episomes promotes rapid reduction in episome numbers and emergence of latent integrants. *Carcinogenesis* 2006;27:2341–53.
18. White JS, Weissfeld JL, Ragin CCR, et al. The influence of clinical and demographic risk factors on the establishment of head and neck squamous cell carcinoma cell lines. *Oral Oncol* 2007;43:701–12.
19. Balló H, Koldovsky P, Hoffmann T, et al. Establishment and characterization of four cell lines derived from human head and neck squamous cell carcinomas for an autologous tumor-fibroblast in vitro model. *Anticancer Res* 1999;19:3827–36.
20. Steenbergen RD, Hermsen MA, Walboomers JM, et al. Integrated human papillomavirus type 16 and loss of heterozygosity at 11q22 and 18q21 in an oral carcinoma and its derivative cell line. *Cancer Res* 1995;55:5465–71.
21. Bouvard V, Storey A, Pim D, et al. Characterization of the human papillomavirus E2 protein: evidence of trans-activation and trans-repression in cervical keratinocytes. *EMBO J* 1994;13:5451–9.
22. de Roda Husman AM, Walboomers JM, van den Brule AJ, et al. The use of general primers GP5 and GP6 elongated at their 3' ends with adjacent highly conserved sequences improves human papillomavirus detection by PCR. *J Gen Virol* 1995;76(Pt 4):1057–62.
23. Weissenborn SJ, Funke AM, Hellmich M, et al. Oncogenic human papillomavirus DNA loads in human immunodeficiency virus-positive women with high-grade cervical lesions are strongly elevated. *J Clin Microbiol* 2003;41:2763–7.
24. Weissenborn SJ, Wieland U, Junk M, et al. Quantification of beta-human papillomavirus DNA by real-time PCR. *Nat Protoc* 2010;5:1–13.
25. .Map Viewer. Available at: http://www.ncbi.nlm.nih.gov/mapview. Accessed on 15 September 2013.
26. Hopman AHN, Smedts F, Dignef W, et al. Transition of high-grade cervical intraepithelial neoplasia to micro-invasive carcinoma is characterized by integration of HPV 16/18 and numerical chromosome abnormalities. *J Pathol* 2004;202:23–33.
27. Olthof NC, Speel E-JM, Kolligs J, et al. Comprehensive analysis of HPV16 integration in OSCC reveals no significant impact of physical status on viral oncogene and virally disrupted human gene expression. *PLoS One* 2014;9:e88718.

28. Smedts F, Schrik M, Horn T, et al. Diagnostic value of processing cytologic aspirates of renal tumors in agar cell (tissue) blocks. *Acta Cytol* 2010;54:587–94.
29. Hafkamp HC, Manni JJ, Haesevoets A, et al. Marked differences in survival rate between smokers and nonsmokers with HPV 16-associated tonsillar carcinomas. *Int J Cancer* 2008;122:2656–64.
30. Lopez JR, Claessen SMH, Macville MVE, et al. Spectral karyotypic and comparative genomic analysis of the endocrine pancreatic tumor cell line BON-1. *Neuroendocrinology* 2010;91:131–41.
31. .Basic Logical Alignment Search Tool (BLAST). Available at: http://blast.ncbi.nlm.nih.gov. Accessed on 13 September 2013.
32. Luft F, Klaes R, Nees M, et al. Detection of integrated papillomavirus sequences by ligation-mediated PCR (DIPS-PCR) and molecular characterization in cervical cancer cells. *Int J Cancer* 2001;92:9–17.
33. Ganguly N, Parihar SP. Human papillomavirus E6 and E7 oncoproteins as risk factors for tumorigenesis. *J Biosci* 2009;34:113–23.
34. Narisawa-Saito M, Kiyono T. Basic mechanisms of high-risk human papillomavirus-induced carcinogenesis: roles of E6 and E7 proteins. *Cancer Sci.* 2007;98:1505–11.
35. Ragin CCR, Reshmi SC, Gollin SM. Mapping and analysis of HPV16 integration sites in a head and neck cancer cell line. *Int J Cancer* 2004;110:701–9.
36. Akagi K, Li J, Broutian TR, et al. Genome-wide analysis of HPV integration in human cancers reveals recurrent, focal genomic instability. *Genome Res* 2014;24:185–99.
37. Lace MJ, Anson JR, Klussmann JP, et al. Human papillomavirus type 16 (HPV-16) genomes integrated in head and neck cancers and in HPV-16-immortalized human keratinocyte clones express chimeric virus-cell mRNAs similar to those found in cervical cancers. *J Virol* 2011;85:1645–54.
38. Huebbers CU, Preuss SF, Kolligs J, et al. Integration of HPV6 and downregulation of AKR1C3 expression mark malignant transformation in a patient with juvenile-onset laryngeal papillomatosis. *PLoS One* 2013;8:e57207.
39. Wiest T, Schwarz E, Enders C, et al. Involvement of intact HPV16 E6/E7 gene expression in head and neck cancers with unaltered p53 status and perturbed pRb cell cycle control. *Oncogene* 2002; 21:1510–7.
40. Yoshida T, Sano T, Oyama T, et al. Prevalence, viral load, and physical status of HPV 16 and 18 in cervical adenosquamous carcinoma. *Virchows Archiv* 2009;455:253–9.
41. Li H, Yang Y, Zhang R, et al. Preferential sites for the integration and disruption of human papillomavirus 16 in cervical lesions. *J Clin Virol* 2013;56:342–7.
42. de Boer MA, Jordanova ES, Kenter GG, et al. High human papillomavirus oncogene mRNA expression and not viral DNA load is associated with poor prognosis in cervical cancer patients. *Clin Cancer Res* 2007;13:132–8.
43. Gammoh N, Grm HS, Massimi P, et al. Regulation of human papillomavirus type 16 E7 activity through direct protein interaction with the E2 transcriptional activator. *J Virol* 2006;80:1787–97.
44. Reimers N, Kasper HU, Weissenborn SJ, et al. Combined analysis of HPV-DNA, p16 and EGFR expression to predict prognosis in oropharyngeal cancer. *Int J Cancer* 2007;120:1731–8.
45. Kumar B, Cordell KG, Lee JS, et al. EGFR, p16, HPV Titer, Bcl-xL and p53, sex, and smoking as indicators of response to therapy and survival in oropharyngeal cancer. *J Clin Oncol* 2008;26: 3128–37.